

## Atomistic model for the evaluation of the stability of diamond under uniaxial tensile force

Yoichiro Uemura

*National Institute for Research in Inorganic Materials, 1-1 Namiki, Tsukuba-Shi, Ibaraki 305, Japan*

(Received 30 July 1993)

An atomistic simulation model for evaluating the stability of crystal under uniaxial tensile force is presented for diamond. The method is based upon the tight-binding approximation, and an interatomic potential which explicitly has an additive cutoff term having a directional dependence is proposed. In the static relaxation procedure for this model, a rigid tetrahedron placed at each atomic position is moved toward the equilibrium configuration by six driving forces, where three are translational and three rotational. As a result, there exists a critical strain of the crystal stability under the uniaxial tensile strain of the [111] direction in diamond. In crystals including vacancies, the strength of the crystal decreased as predicted by Griffith's theoretical treatment. The critical strength of the perfect diamond crystal is found to be about 80 GPa. The nonlinear relationship between stress and strain of diamond under larger external forces is obtained from the results for equilibrium states. The functional form in a cubic polynomial of strain reproduces very well the calculated plots.

### I. INTRODUCTION

The stability of crystal under an external force is a very important problem in the engineering materials and this provides some information for crack propagation or fracture in crystals. In highly covalent crystals which are expected to be used as structural materials, fracture characteristics play dominant roles in the applicability for practical uses. A theoretical approach to this problem is important for designing the materials having various physical properties. In the early stage, crystal stability had been discussed in terms of theoretical strength<sup>1,2</sup> or as the problem of ductile-brittle behavior.<sup>3,4</sup> Later, there have been many attempts for studying mechanical properties or coordination configurations of covalent crystals by atomistic simulation models using empirical interatomic potentials.<sup>5-9</sup> Sinclair reported the atomistic model of crack propagation in covalent crystal with the boundary condition as being joined to the continuum model region<sup>10</sup> and examined the effect of interatomic potential form on crack propagation.<sup>11</sup> A bond breakage means the generation of dangling bonds and is an essential problem in fracture of crystalline materials. However, the treatments have been complicated in the previous reports in which the bond tension or the bond strain have been employed as a cutoff parameter.

In the atomistic model simulations of macroscopic phenomena such as crack propagation or fracture, the number of atoms included in calculation would be necessarily rather great.<sup>11</sup> At the present stage, this demand could not be satisfied in the model with the complex potentials or with rather complicated calculation procedures in molecular dynamics, although some complications could not be avoided in the treatment of the covalent crystal because of its strong anisotropic bond character.

In this work, a simple atomistic model for evaluating the stability of covalent crystals under uniaxial external tensile force is proposed. The interatomic potential<sup>12</sup> is

based upon the tight-binding approximation model considering only nearest neighbor interaction.<sup>5,13</sup> And an extra term responsible for generating the dangling bonds is added to this potential. The relaxation procedure is performed by translation and rotation of the rigid tetrahedron placed at each atomic site. And the model is applied to investigate the stability of diamond as typical of a covalent crystal. How the vacancies introduced in crystals affect the stability of crystal will also be evaluated.

### II. METHOD OF CALCULATION

#### A. Potential and relaxation procedure

In the tight-binding approximation, an interatomic potential is given as the interaction of  $sp^3$  hybrid orbitals of connecting atoms. A total energy of the system,  $E_{\text{total}}$ , is

$$E_{\text{total}} = \sum_i E_i,$$

$$E_i = \frac{1}{2} \sum_j V_{ij}, \quad j = 1, 2, 3, 4,$$

$$V_{ij} = -\{F(R, P_i, P_j, P_{ij}) + E_{\text{dang}}\},$$

where  $E_i$  is a site energy of site  $i$ ,  $V_{ij}$  is a pair potential, and  $F(R, P_i, P_j, P_{ij})$  is a bond energy of the tight-binding approximation<sup>13</sup> with Slater-Koster terms which depend on the bond directions.<sup>14</sup> The distance between interacting atoms is denoted by  $R$ . The terms  $P_i$ ,  $P_j$ , and  $P_{ij}$  are the variables for the direction of interacting orbitals of the atoms  $i$  and  $j$  as follows:

$$P_i = ll_i + mm_i + nn_i,$$

$$P_j = ll_j + mm_j + nn_j,$$

$$P_{ij} = l_i l_j + m_i m_j + n_i n_j,$$

where  $(l_i, m_i, n_i)$  and  $(l_j, m_j, n_j)$  are the directions of the

interacting orbitals of each atom, and  $(l, m, n)$  is the direction cosine of the bonding axis between two atoms. The parameters in the function  $F$  are determined from bulk modulus, cohesive energy, and equilibrium condition of crystal.<sup>13</sup>

The function  $F(R, P_i, P_j, P_{ij})$  shows the asymptotic behavior with an increase in atomic distance to the hybrid energy which is approximated by the dangling bond energy here. It never reaches, however, the value at a finite distance. For creation of a dangling bond at a finite distance, a certain function should be introduced into the bond energy  $V_{ij}$ . It would be plausible to employ a function which depends upon the deviation of angle of interacting orbitals  $P_i$  and  $P_j$  because of the strong directional bonding character of covalent crystals. The function  $E_{\text{dang}}$  in additive form is introduced to see its effect on fracture behavior. So far there has been no proposal as to the functional form of such a function. As a first approximation,  $E_{\text{dang}}$  is postulated in a simple form as follows:

$$E_{\text{dang}} = \alpha(1 + P_i P_j).$$

This is the same as a  $\pi$ -like interaction of the Slater-Koster terms present in function  $F$  without exponential decay factor, where the constant  $\alpha$  is determined from the condition that  $V_{ij}$  should be equal to twice the value of hybrid energy when the bond is ruptured. It is also postulated that bond breakage will occur when two interacting orbitals of adjacent atoms deviate beyond a critical angle  $\theta_c$  defined as follows:

$$\cos\theta_c = R_c / (R_c^2 + R_0^2)^{1/2}.$$

The situation is shown in Fig. 1, where the direction of the bonding axis at equilibrium in a perfect crystal is  $\zeta$  and the atomic distance is  $R_0$ , and the plane perpendicular to the  $\zeta$  axis is indicated as the  $\xi\eta$  plane and  $R_c$  is a critical distance in that plane.  $R_c$  is an arbitrary cutoff parameter reflecting a rigidity of the material, and its value is adopted here to be between 0.2 and 0.4 without physical rationalization. It is a characteristic assumption in this model that the cutoff length depends upon the deviation in orbital directions of the interacting atoms. Schematic potentials are illustrated in Fig. 2 for different values of deviation in the  $\xi\eta$  plane.

The hybrid orbitals of  $sp^3$  form a tetrahedron whose center is an atomic site, and each orbital is directed to the

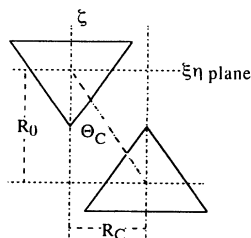


FIG. 1. Critical configuration at which bond breakage takes place.

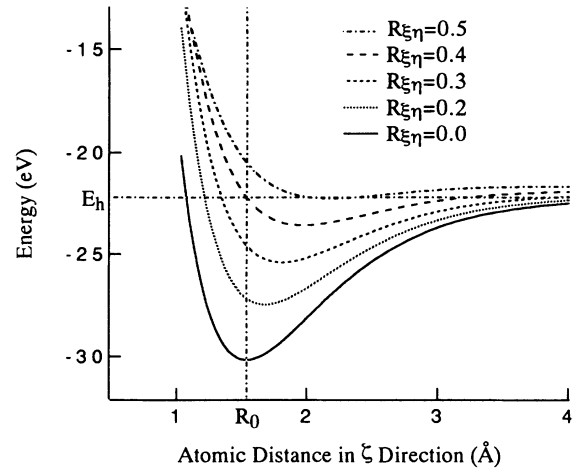


FIG. 2. Interatomic potential for some parameter values representing the deviation of bond direction where  $R_c$  is 0.4.

top of the tetrahedron. Only the nearest-neighbor interactions are considered in the present model, and it is assumed that a tetrahedron behaves as a rigid body in the process of relaxation. It is displaced by three translation forces and rotated by three independent torques. This model would be referred to as a “rigid tetrahedron model.” The rigidity of the tetrahedron is sustained by keeping the orthonormality condition of each hybrid orbital through the relaxation process. This assumption might be rather artificial but it reduces the number of calculation parameters and would enable the construction of an atomistic model for evaluating the crystal stability with a considerable number of atoms.

A net force,  $G_i$ , acting on atom  $i$  is defined as follows:

$$G_i = \left[ \sum (F_k^2 + T_k^2) \right]^{1/2}, \quad k = 1, 2, 3,$$

where the torque,  $T_k$ , means the differential of the potential with respect to the appropriate three components among the expanding coefficients of the four hybrid orbitals by  $s$  and  $p$  atomic orbitals. It can be considered that this quantity is a measure of instability of the atomic site. When the maximum net force,  $G_{\text{max}}$ , among  $G_i$  of all atoms becomes smaller than the tolerance ( $5 \times 10^{-3}$  eV/Å or  $8 \times 10^{-7}$  dyn), the configuration is considered to be the equilibrium.

## B. Boundary and initial conditions

Because a covalent crystal has a very strong anisotropic character, bonding direction and rotation angles should be referred to the fixed coordinate axes in the relaxation calculation. Three axes of Cartesian coordinates are taken as corresponding to the crystallographic principal axes of diamond structure;  $x$  is  $[11\bar{2}]$ ,  $y$  is  $[\bar{1}10]$ , and  $z$  is  $[111]$ , which is the direction of uniaxial strain. The nearest atomic distance in the  $(111)$  plane is taken to be unity in this calculation. A periodic boundary condition can be adopted in the  $y$  direction because of crystal sym-

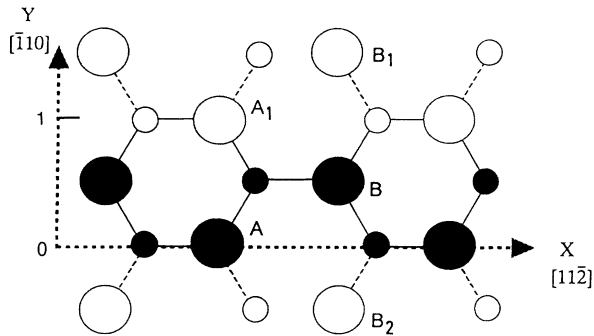


FIG. 3. Atomic configuration in the (111) plane indicating a periodic boundary condition in the  $y$  direction.

metry and we choose the minimum period ( $=1$ ) as the width of the crystal in the  $y$  direction (Fig. 3). The solid and open circles indicate the atoms belong to the region of relaxation and the adjacent atoms, respectively. The small circles correspond to the atoms on the different planes from large ones with respect to the  $[111]$  direction. The atoms  $A$  and  $A_1$  are relaxed in the same coordinates of the  $x$  and  $z$  directions while their distance in the  $y$  direction is fixed to be unity. In the same manner,  $B_1$  and  $B_2$  are related by periodic boundary conditions to atom  $B$ . When a point defect is introduced in a crystal, it means a line defect in the  $y$  direction. In the  $z$  direction, which is considered as a layer structure, the numbers  $L=1$  and  $L_{\max}$  correspond to the two opposing outermost layers. The  $z$  coordination of  $L=1$  is taken to be 0 and the  $L_{\max}$  is always taken to be a multiple of 6 which is the periodicity in the  $z$  direction of a perfect diamond structure. The boundaries of the  $z$  direction are terminated by fixed atoms. On the other hand, because of lacking any symmetry in the  $x$  direction, two extreme boundary conditions (fixed and free) are adopted in this direction. In the case of a free boundary condition, the atoms at the outermost sites in the  $x$  direction have dangling bonds initially.

In the present model, the strain of the  $z$  direction is adopted as an external force parameter instead of  $[111]$  tensile stress. The calculation is initiated by giving a finite tensile strain, then all of atoms including just outside atoms are uniformly displaced in the  $z$  direction. The strain in the  $z$  direction,  $S$ , is defined as  $S = \Delta Z / Z_0$ , where  $\Delta Z = Z_{\max} - Z_0$ ,  $Z_0$ , and  $Z_{\max}$  are crystal thicknesses in the  $z$  direction without and with external strain, respectively. The region of calculation is a rectangular form, while it extends infinitely in the  $y$  direction.

When the vacancies are introduced, the calculation region in the  $x$  direction is divided into the two parts. Region I, which has the size of  $l_c$ , corresponds to a vacancy region and region II is the same as perfect. The origin of the  $x$  direction is taken at the boundary between the two regions. The middle level in the  $z$  direction is set at midline between  $L_{\text{vac}} (= L_{\max} / 2 + 1)$  and  $L_{\text{vac}} - 1$ , and is termed midplane, where the vacancies are introduced on the layer  $L_{\text{vac}}$ .

### III. RESULTS

#### A. Perfect crystal

The atoms which are initially displaced uniformly by smaller  $S$  in the  $z$  direction are found to be slightly relaxed toward the opposite directions whose layers are an odd number (positive direction in  $z$ ) or even number (negative). And finally the equilibrium configuration is attained when the net force acting on each atom is smaller than the tolerance except for those acting on the fixed boundary atoms in the case of a fixed boundary condition.

On the other hand, in the case of a larger strain, the status is quite different. As an example of this situation, the maximum net force  $G_{\max}$  as a function of iteration number is shown in Fig. 4 with that for the stable state. The calculation parameters of this case are as follows:  $L_{\max} = 48$ ,  $X_{\max} = 17$ ,  $R_c = 0.4$ ,  $S = 0.184$  for a stable state and  $S = 0.263$  for an unstable state under a free boundary condition in the  $x$  direction. The stability of crystal under tensile stress depends on the magnitude of strain provided initially and it indicates the existence of critical strain,  $S_c$ .  $S_c$  for the perfect diamond crystal is found to be  $0.187 \pm 0.003$  for this boundary size in which about 4000 atoms are contained. The atomic structures and their energies for an unstable state ( $S = 0.263$ ) are shown in Fig. 5 at several iteration numbers where each stage is shown in Fig. 4. The diameter of the circles at each site is roughly proportional to the magnitude of the site energy. The minimum circles indicate the atoms which have negligibly small excess energies. The maximum circles correspond to the atoms whose energies are larger than twice the value of dangling bond energy. The energies caused by the dangling bond in the  $z$  direction are omitted from the site energies of the atoms on  $L=1$  and  $L_{\max}$  layers in this figure. At the stage of Fig. 5(a), the distance of the interlayer is extended at each six layers reflecting the periodicity of the  $[111]$  direction. With the progress in iteration, however, the periodicity of the extended layer seems to change to 12, and the energies of the sites facing to extended planes increase because of dangling bond generation. It should be noted that these

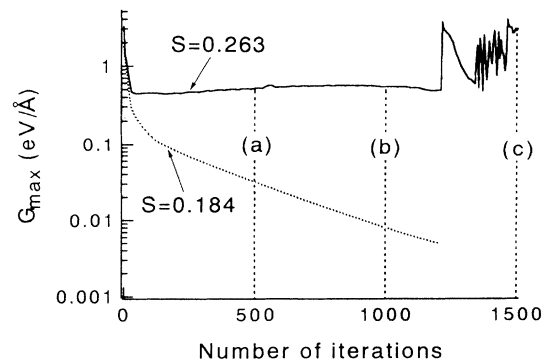


FIG. 4. Maximum net force vs number of iterations for the perfect crystal under the free boundary condition. The region size is  $X_{\max} = 17$  and  $L_{\max} = 48$ .

situations do not simulate accurately the behavior of fracture with molecular dynamics because the present treatment is a static relaxation method. However, if the simultaneous displacement in the  $z$  direction of all atoms by external tension is assumed, these features would give a rough sketch for the process of fracture. It seems that the voids appear at the boundary and they behave as

open cracks. The relaxation process under the fixed boundary condition in the  $x$  direction has also been calculated. The results are shown in Figs. 6 and 7 for the same calculation parameters as those of Fig. 5. Each iterative stage of Fig. 7 is represented in Fig. 6. The extension of an interlayer begins at the neighborhood of the boundaries but the voids stay closed because the edge

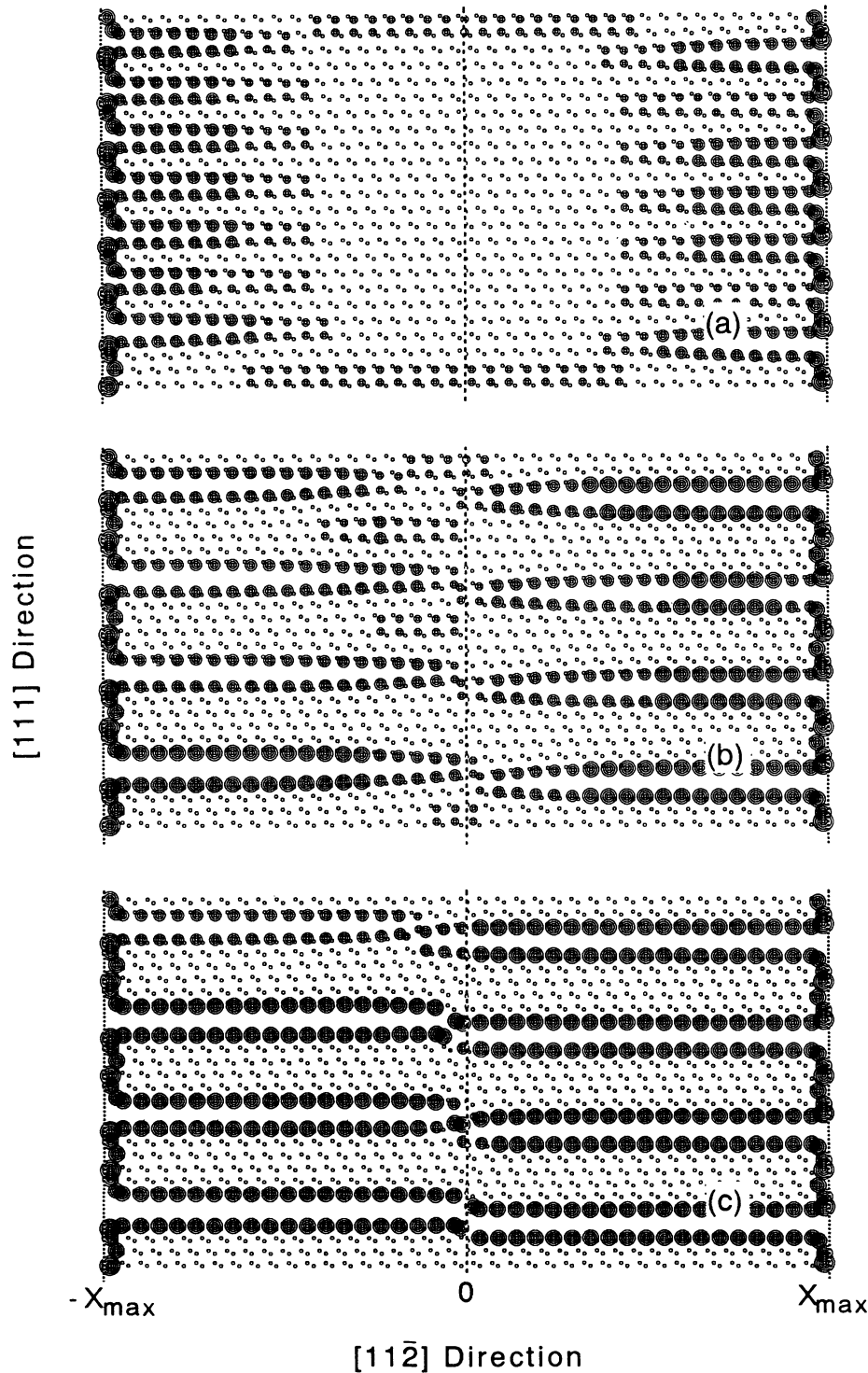


FIG. 5. Atomic structure and energy diagram at several iteration stages for the unstable state of the perfect crystal under a free boundary condition. Each stage corresponds to the iteration number denoted in Fig. 4.

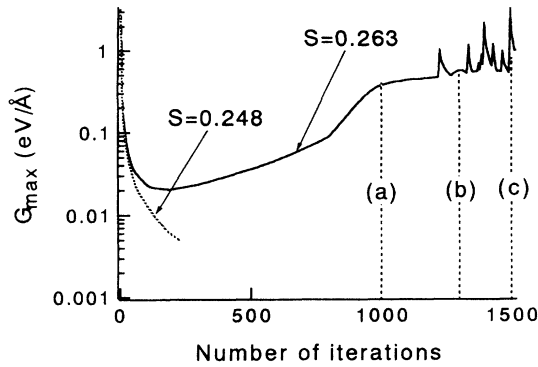


FIG. 6. Maximum net force vs number of iterations for the perfect crystal under a fixed boundary condition. The region size is  $X_{\max} = 17$  and  $L_{\max} = 48$ .

atoms are fixed. The critical strain for this case is found to be  $0.256 \pm 0.003$ , which is rather larger than the value for a free boundary condition. This suggests that the boundary condition should be carefully considered for the evaluation of the strength of a perfect crystal.

The boundary size might also affect the feature of fracture of crystal. The critical strains are evaluated for the boundary sizes of ( $X_{\max} = 32$ ,  $L_{\max} = 48$ ) and ( $X_{\max} = 32$ ,  $L_{\max} = 60$ ) under a fixed boundary condition. The values of the  $S_c$  are  $0.256 \pm 0.003$  for the former and  $0.255 \pm 0.004$  for the latter, and the numbers of atoms included in these regions are about 7300 and 9000, respectively. The critical strain does not depend on boundary size, and the feature of the unstable state for three kinds of the boundary size resemble fundamentally each other. The atomic structure and their energies calculated by a fixed boundary condition for the unstable state ( $S = 0.261$ ) with greater region size ( $X_{\max} = 32$ ,  $L_{\max} = 60$ ) is shown in Fig. 8.

### B. Introduction of point vacancy

If the cluster length  $l_c$ , which is the width of region I, is taken to be 1, the only one site exists on a vacancy layer. Then the only one atom is removed from the  $L = L_{\text{vac}}$  layer (it is 25 when  $L_{\max} = 48$ ) creating point vacancy and the midplane of the  $z$  direction is located midway between  $L = 24$  and 25. When a smaller strain is given uniformly to this lattice, most of the atoms are relaxed, as in the case of the perfect crystal, while some atoms in the neighborhood of the vacancy move increasing the vacancy volume as shown in Fig. 9. The calculation parameters are as follows: boundary size is ( $X_{\max} = 17$ ,  $L_{\max} = 48$ ),  $l_c = 1$ ,  $R_c = 0.4$ , and  $S$  is 0.148 under the free boundary condition. An asterisk indicates the vacancy position and the sites  $A$ ,  $B$ , and  $C$  are nearest-neighbor atoms of the vacancy. The energy of atom  $A$  is larger than the others because it has two dangling bonds. On the other hand, the status is different from that of the perfect crystal in the case of the larger strain,  $S = 0.158$ .  $G_{\max}$  as a function of the number of iterations is shown in Fig. 10 with that of the stable state. The value of critical strain,  $S_c$ , is found to be  $0.151 \pm 0.003$ , which is smaller

than the value for the perfect crystal, meaning a reduction in strength. At the early stages of iterations,  $G_{\max}$  for the unstable state decreases like that of the stable state. Before it converges to a negligibly small value, however, it begins to increase. And at a certain stage, the bonds of some atoms facing the opposite side of the midplane are ruptured generating dangling bonds in pairs. The atomic structures and their energies for the unstable state ( $S = 0.158$ ) are shown in Fig. 11 for several stages indicated in Fig. 10. With the progress in iteration, the number of atoms having the dangling bond increases and finally the crack reaches both crystal edges which means the fracture of the crystal. This situation displays the crack propagation or the cleavage along the (111) plane of the diamond crystal by a large external tensile force.

The diagrams of the net force acting on each atom,  $G_i$ , are shown in Fig. 12 at the stages corresponding to Fig. 11. The diameter of the site indicates the instability of the atom. It can be seen that the unstable atoms concentrate near both edges of the void with the progress in iteration. This may correspond to the stress concentration at the crack edge treated in linear elastic theory.

The effect of the boundary condition and of the calculation size on  $S_c$  are examined. In this case, any clear difference in  $S_c$  cannot be observed by the changes of the boundary conditions (fixed or free) and of the region sizes ( $X_{\max} = 17$ ,  $L_{\max} = 48$ ), ( $X_{\max} = 32$ ,  $L_{\max} = 48$ ), and ( $X_{\max} = 30$ ,  $L_{\max} = 60$ ).

### C. Pairing of two vacancies

Aggregate of vacancies is termed vacancy cluster. The larger size of the calculation region should be necessary for the larger-scale clusters. Only small size clusters consisting of pairs of two vacancies are considered in this paper. There are two typical ways to form the cluster by a pair of two vacancies. One is a linkage in the  $[111]$  direction and the other is in the  $[1\bar{1}2]$  direction. The former is termed longitudinal and the latter transverse.

We have special interests in the vacancy clusters aggregated in the (111) plane (transverse type) because they will be able to simulate the (111) crack or cleavage in the diamond crystal. In this model, the cluster size of the two vacancies in transverse type can be given by twice of region I of the point vacancy. This procedure increases the number of vacancies and total number of atoms under consideration if the size of region II is fixed. The atomic structures and their energies in the case of the vacancy cluster length,  $l_c = 2$ , which means the transverse mode, are shown in Fig. 13 at a certain stage of iterations for the unstable state ( $S = 0.142$ ). The calculation parameters are the same as those of the point vacancy except  $l_c = 2$  under the free boundary condition. The critical strain of the transverse mode is found to be  $S_c = 0.124 \pm 0.003$ , which is smaller than the value for the point vacancy.

On the other hand, for the creation of the longitudinal cluster composed of two vacancies, the atoms are removed from the layers  $L = L_{\text{vac}}$  and  $L_{\text{vac}} - 1$  in region I of  $l_c = 1$ . The critical strain is the same as the value for

the point vacancy,  $S_c = 0.151 \pm 0.003$ . The atomic structure and their energies are shown in Fig. 14 for the same strain as the value for the case of the transverse ( $S = 0.142$ ). For the same value of the strain, the former reaches an equilibrium state while the later shows crack propagation. The reason why the critical strain of the

longitudinal mode is larger than that of the transverse mode may be due to a smaller number of dangling bonds at an initial state. And this result agrees qualitatively with Griffith's macroscopic treatment<sup>15</sup> in which the critical strength of the crystal decreases with increase of the crack length.

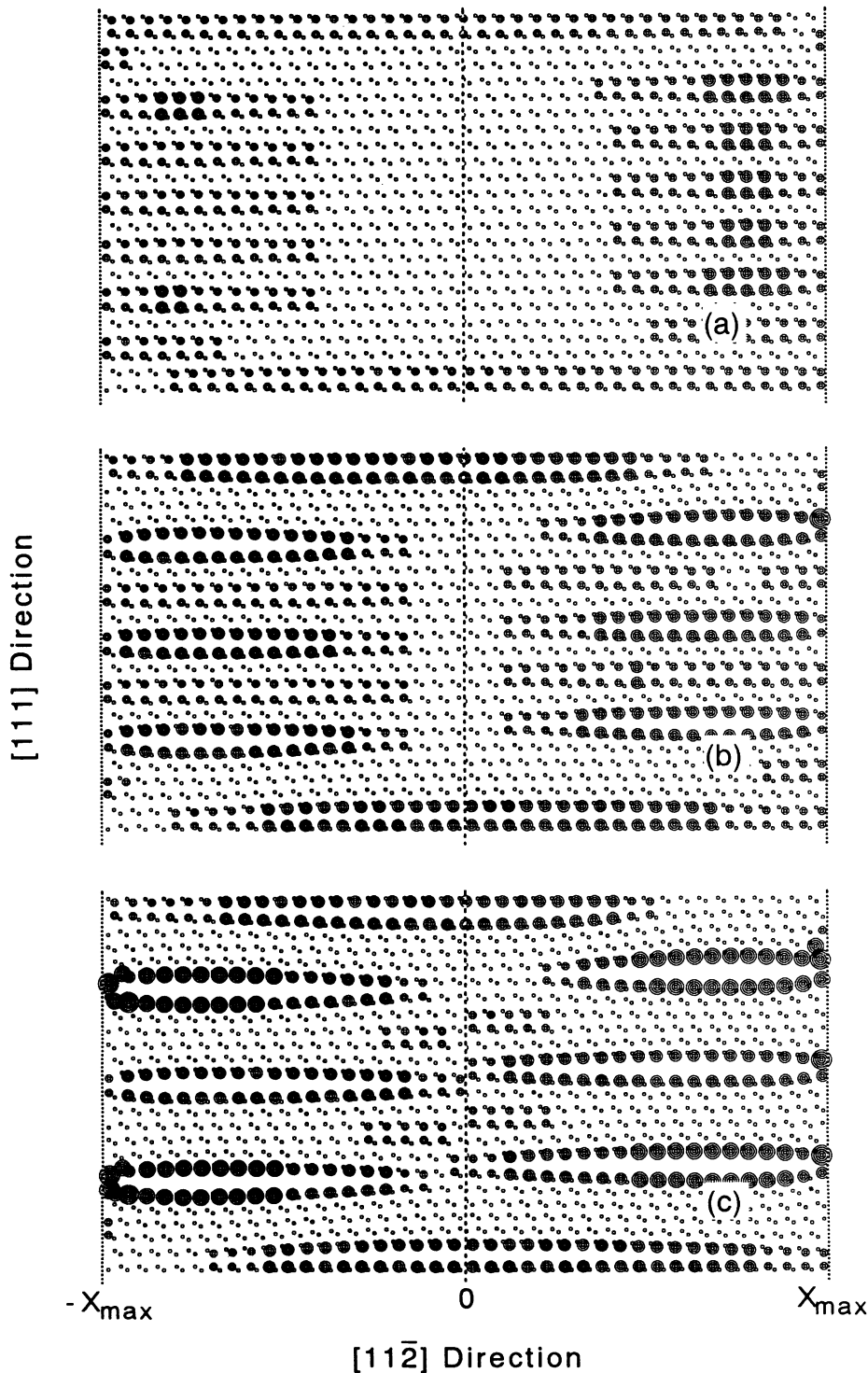


FIG. 7. Atomic structure and energy diagram at several iteration stages for an unstable state of the perfect crystal under a fixed boundary condition. Each stage corresponds to the iteration number denoted in Fig. 6.

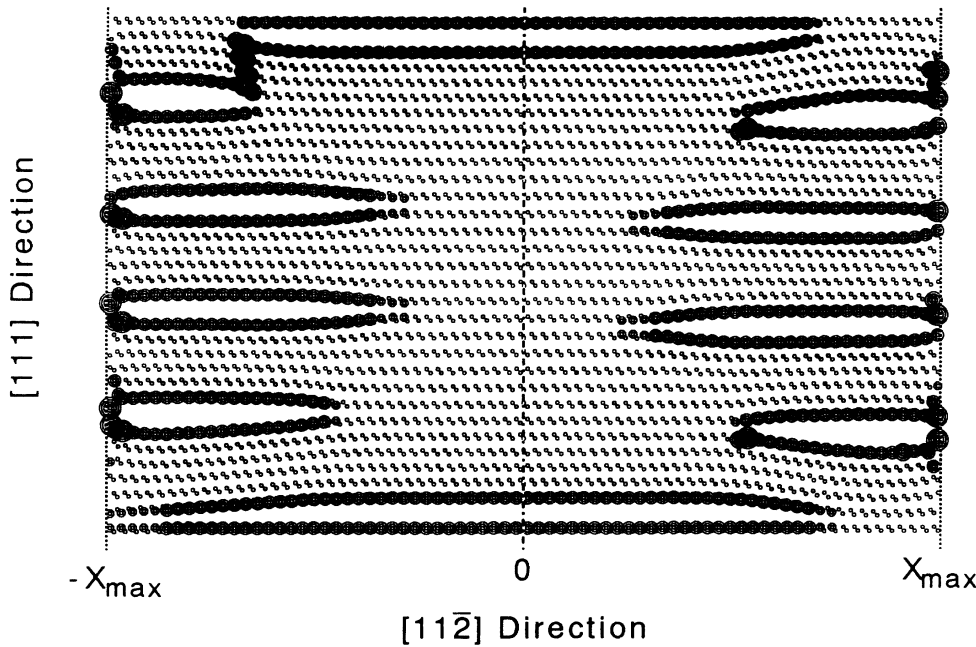


FIG. 8. Atomic structure and energy diagram at iteration number = 2000 for an unstable state ( $S=0.261$ ) of the perfect crystal under a fixed boundary condition. Where  $R_c=0.4$  and the region size is  $X_{max}=32$ ,  $L_{max}=60$ .

**D. The relationship between stress and strain**

The internal stress distribution of the unstable state is presented for the case of the point vacancy in Fig. 12. At the equilibrium, all of the net forces acting on the atoms in the internal region tend to be negligibly small, while the forces acting on the fixed atoms on the boundary layers in the  $z$  direction remain to have finite values. The sum of these forces in the  $z$  direction is considered a tensile external force which gives the initial strain. A virtual external stress in the  $[111]$  direction,  $\sigma_{111}$ , will be formally obtained with the total force acting on the outer layer divided by the surface area as follows:

$$\sigma_{111} = \sum Fz_i / (N \times S_a),$$

where  $N$  is a number of atoms on the  $L = 1$  layer and  $S_a$

is an atomic area in the  $(111)$  plane which is  $5.41(\text{\AA}^2)$  for diamond.

The tendency of  $\sigma_{111}$  with the progress in iteration is shown in Fig. 15 for the stable ( $S=0.148$ ) and the unstable ( $S=0.158$ ) cases for the point vacancy system under the free boundary condition. The curve for the unstable state shows a plateau and then decreases and this might reflect the starting of crack propagation. On the contrary, the curve for the stable state converges to a certain value,  $\sigma_{111}^*$ , by the achievement of equilibrium. The relationship between initial strain and the corresponding convergent value  $\sigma_{111}^*$  for some equilibrium states are shown in Fig. 16 with the values for the perfect and those for the pair of vacancies in the transverse mode. The vacancies

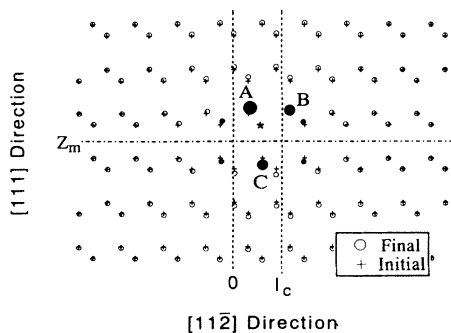


FIG. 9. Atomic structure at a neighborhood of a point vacancy at equilibrium for  $S=0.148$ .

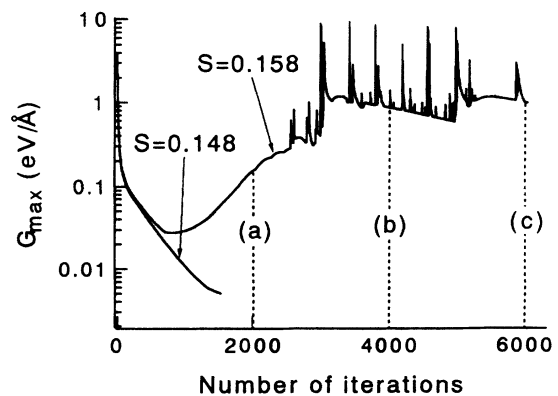


FIG. 10. Maximum net force vs number of iterations for the crystal including a point vacancy under a free boundary condition. The region size is  $X_{max}=17$  and  $L_{max}=48$ .

influence the crystal strength, but they do not practically affect the relationship between stress and strain. The straight line obtained from the experimental value of the elastic stiffness constant of diamond,<sup>16</sup>  $C_{11} = 6.7$  (eV/Å<sup>3</sup>), and the best-fit curve to the calculated points are also shown in the figure. The result of the best-fit procedure indicates the nonlinear form of a cubic polynomial as follows:

$$\sigma_{111}^* = 5.0S(1 - 1.3S)^2.$$

The coefficient of the linear term,  $5.0$  (eV/Å<sup>3</sup>), is a little smaller than the above cited one. The value of  $C_h$ , which is the critical strength of the perfect diamond crystal, is  $0.5$  (eV/Å<sup>3</sup>) =  $80(10^{10} \text{ dyn cm}^{-2}) = 80 \text{ GPa}$ , and it is smaller than the value of the theoretical tensile strength,  $106$  ( $10^{10} \text{ dyn cm}^{-2}$ ), reported by Tyson.<sup>1</sup>

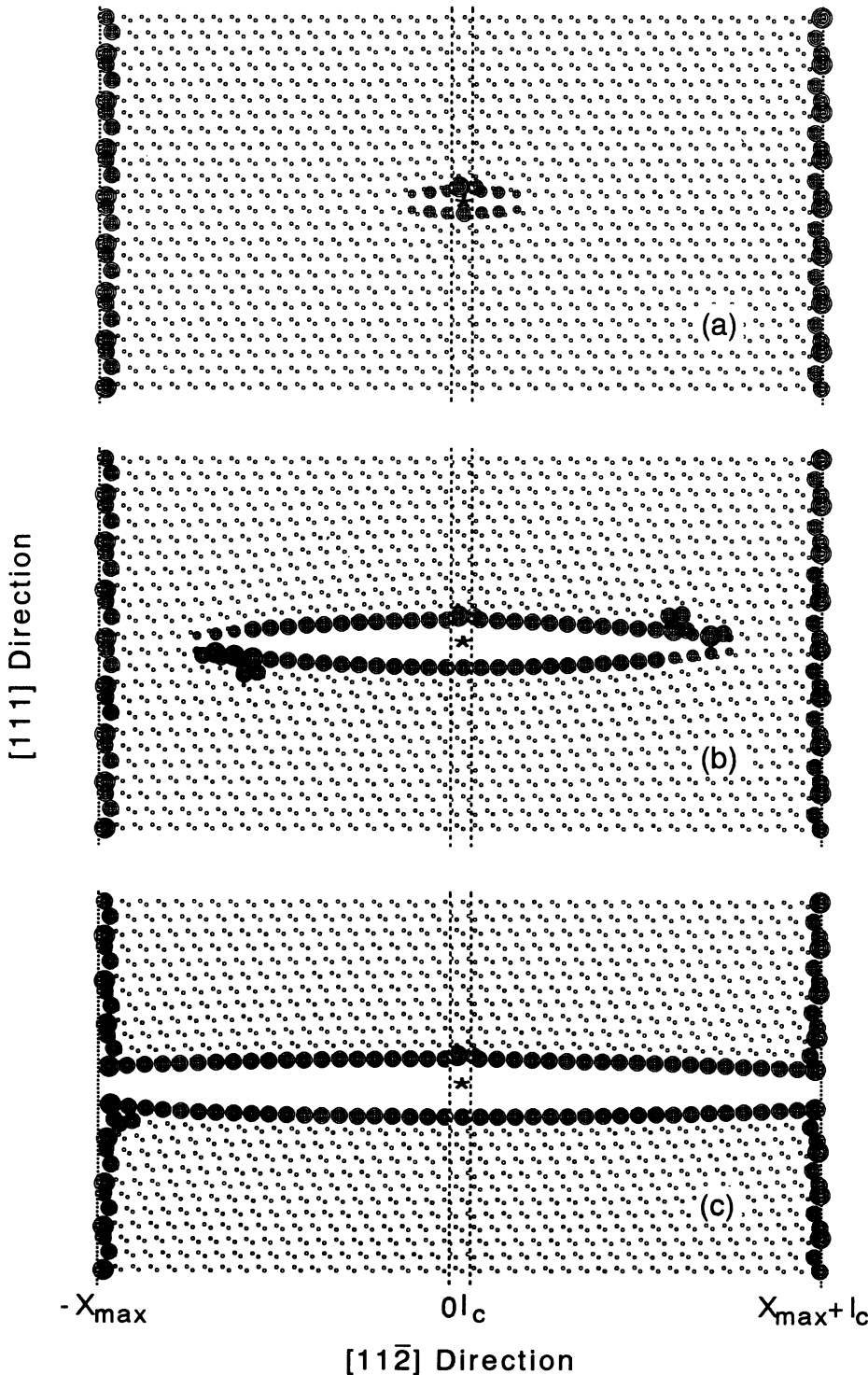


FIG. 11. Atomic structure and energy diagram at several iteration stages for an unstable state of the crystal including a point vacancy under a free boundary condition. Each stage corresponds to the iteration number denoted in Fig. 10.



## IV. DISCUSSION

The stability of the diamond crystal under the external tensile force has been evaluated by using the "rigid tetrahedron model" with the interatomic potential including the extra term for cutoff. In the present model, there are several assumptions at some calculation stages. The first basic problem is the form of the term  $E_{\text{dang}}$  in

the potential function. In most of the reports concerning this subject,<sup>7,8,9,11</sup> however, the authors proposed the cutoff functions and the cutoff lengths in rather arbitrary manners. As mentioned above, the  $E_{\text{dang}}$  proposed here is a kind of cutoff function which has directional dependence. This directional dependence of the cutoff length arises from the model of the rigid tetrahedron, and this kind of procedure would be more appropriate for atomis-

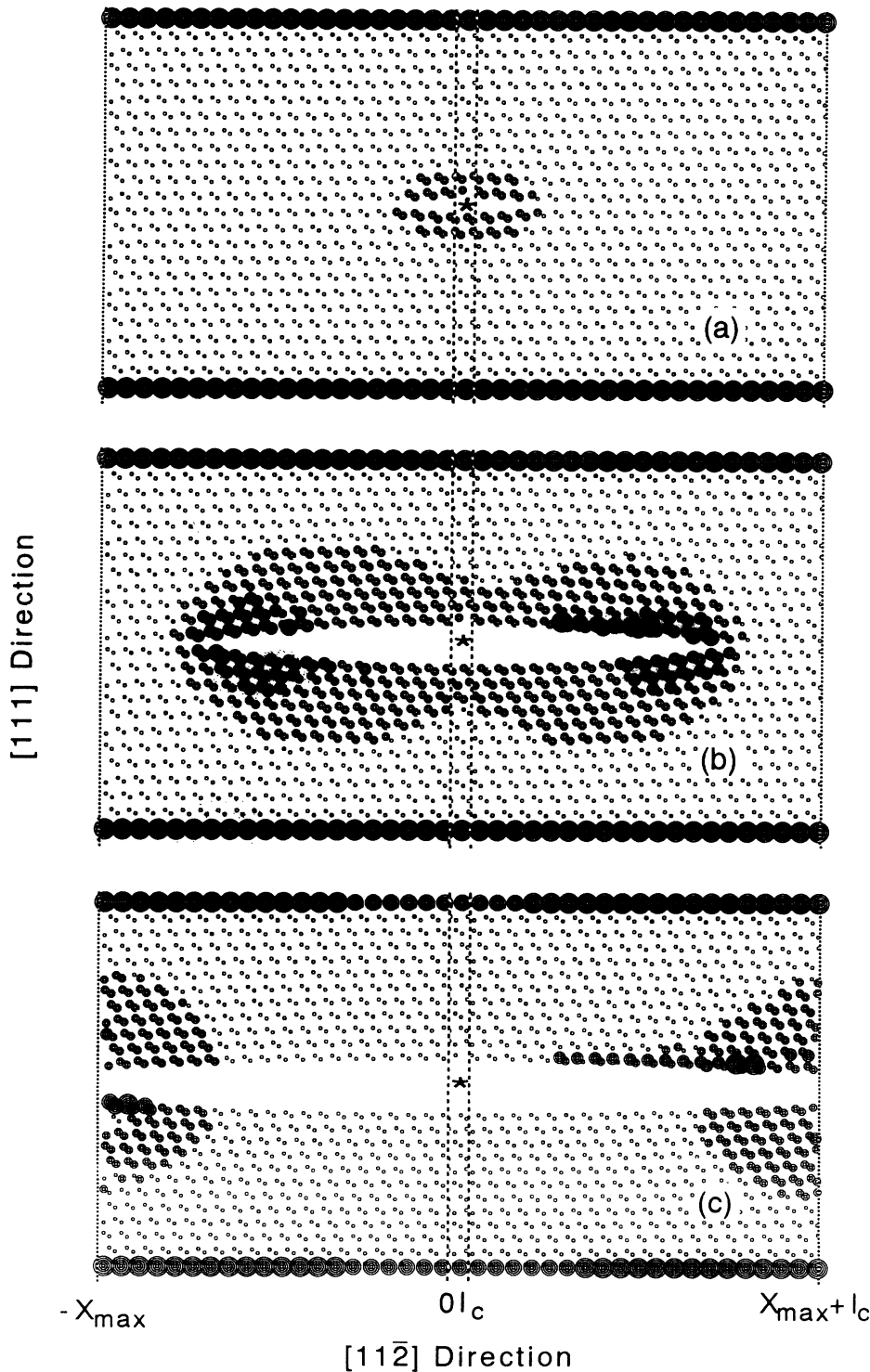


FIG. 12. Atomic structure and net force diagram for the same calculation conditions as those in Fig. 11.

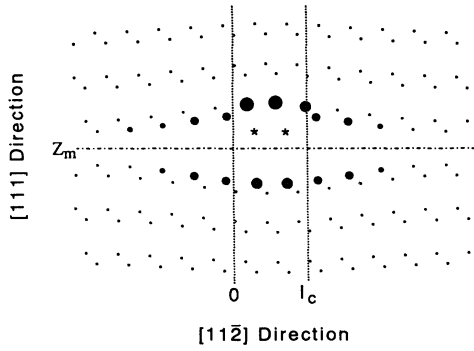


FIG. 13. Atomic structure and energy diagram for the transverse mode of the double vacancies at iteration number=1500 and  $S=0.142$ .

tic simulation for a highly anisotropic crystal. The differentials of this potential, the forces, are discontinuous at the cutoff point. It is pointed out<sup>5</sup> that this situation would be disadvantageous for a molecular-dynamics simulation. Further trials may enable us to find a more appropriate functional form of the cutoff.

The surface reconstruction after generation of dangling bonds could not be discussed here because of the nearest-neighbor approximation. This concept might be necessary for the more detailed discussion, but it can be neglected in the first-order approximation.

A boundary condition is one of the important problems in atomistic model simulation. It has been pointed out<sup>11,17,18</sup> that attention should be paid to the boundary condition between a continuum region and atomistic one. In this model, the outer boundary of region II corresponds to it and atoms placed at just outside the boundary are fixed or removed through a relaxation process depending on the two extreme boundary conditions in the  $x$  direction. The plausible situation might exist in a midway between the two extreme cases. The boundary condition affects the fracture behavior in the case of the perfect crystal because the atoms immediately adjacent to the outer sites of the boundary are practically not in the same condition as the remainder. In contrast, the effect of the boundary condition can be neglected for the crystal

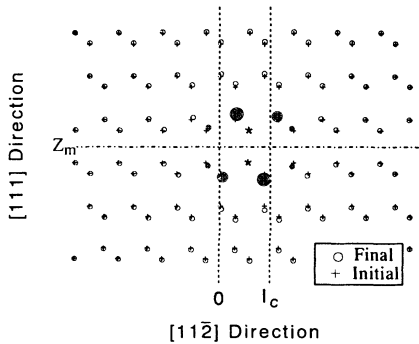


FIG. 14. Atomic structure and energy diagram for the longitudinal mode of the double vacancies at equilibrium (iteration number=1444,  $S=0.142$ ).

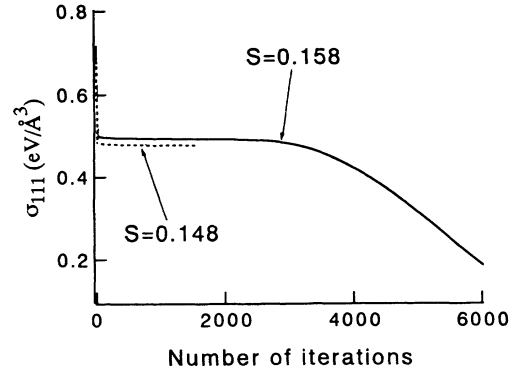


FIG. 15. Virtual external stress vs number of iterations for stable ( $S=0.148$ ) and unstable states ( $S=0.158$ ) of the crystal including point vacancy.

including vacancies. The effect of crystal size,  $X_{max}$  and  $L_{max}$ , on  $S_c$  has also been evaluated for the cases of the perfect crystal and the point vacancy system. The results show that the effect would be negligibly small if it exists. Thus, the boundary size  $X_{max}=17$  and  $L_{max}=48$  has been adopted in present calculations except for special cases. The effect of  $R_c$  on  $S_c$  is also examined for the case of the point vacancy under the free boundary condition. The value of  $S_c$  is almost unchanged from  $R_c=0.2-0.4$ . This means that the coefficient  $\alpha$  in  $E_{dang}$  may not affect seriously the value of critical strain.

When uniaxial external tensile force is applied to a material, Poisson contraction will be an important problem. In the case of the fixed boundary condition in the  $x$  direction here, this effect cannot be expected. On the other hand, it may be worthwhile to evaluate this effect for the case of the free boundary condition. The  $x$  components of the displacement of the atoms on the neighbor layers of midline in the  $z$  direction are examined for the case of the point vacancy. It can be seen in Fig. 9 that the atoms

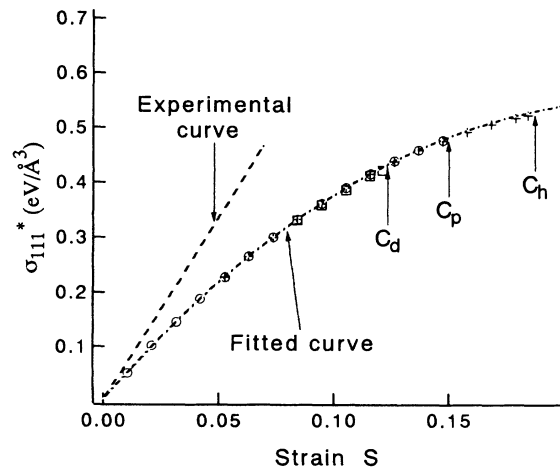


FIG. 16. Convergent external stress vs initial strain for some equilibrium states of the perfect (+), the point vacancy (o), and the double vacancies (□).  $C_h$ ,  $C_p$ , and  $C_d$  represent critical points in respective cases.

in the neighborhood of the vacancy shift along an inward direction from the initial positions while the values of displacement decrease on going away from the center. The strains in the  $x$  direction of the atoms at the outermost region are estimated to be an order of 0.0001 and the directions of displacement are not uniform. These results signify that Poisson contraction does not occur in this model. The reason may be considered that the elongation in the  $z$  direction does not mean the elongation of the bond orbital but the increase of the atomic distance in the rigid tetrahedron model. That is that the extension in a certain direction does not always result in the generation of the driving force and the shortening of the atomic distance in the perpendicular.

The value of the critical strain depends on the initial condition of the atomic configuration. The two kinds of initial configuration are investigated besides the uniform mode which is basically adopted here. One is termed "step mode" which has a sharp step between regions I and II at the initial configuration. All atoms in region II are displaced in the same manner as in the uniform mode, while the atoms in region I are displaced in the opposite direction with respect to the midplane of the  $z$  direction resulting additive distance of  $Z_0$  between  $L_{\text{vac}}$  and  $L_{\text{vac}} - 1$  layers. This mode arises from the consideration that the atoms just on and under the vacancies can move freely because of the lack of bonding. The other is termed "buffer mode" which has a buffer region between regions I and II. The atoms in the buffer region are initially displaced in the quantities depending on the coordinations in the  $(x, z)$  plane. The  $S_c$  of the crystal including the point vacancy are about 0.105 and 0.15 for the step mode and the buffer mode of buffer size 2, respectively. The  $S_c$  for the uniform mode is 0.151. The uniform mode might be the best initial condition in the present model and this mode has been adopted here.

The critical strength evaluated here for the perfect diamond crystal is smaller than the theoretical value reported,<sup>1</sup> but it is still larger than the recent experimental value.<sup>19</sup> The result that the critical strength decreases with the increase of the number of vacancies might suggest the possibility of evaluating Griffith's relation between the crack length and the crystal strength in the atomistic level. For this purpose, a wider calculation region and a longer vacancy cluster length should be examined. And the enlargement of calculation region will also be necessary for the atomistic evaluation of correlation between the crystal stability and the various imperfections of the crystal.

The nonlinearity in the relation between stress and strain obtained in this work seems to be unusually large for diamond which is believed to be very rigid and does not show clear dislocation movement or plasticity in fracture.<sup>20</sup> It is considered that the cause of this discrepancy might be responsible for the interatomic potential, especially the cutoff term.

There are many reports about a molecular-dynamics (MD) simulation for isotropic materials like some metals or inert-gas solids in which the interatomic potential depends only on the interatomic distance. It can be said that the "rigid tetrahedron model" is an initial step for MD simulation of macroscopic properties like fracture toughness for crystals which have strong anisotropic bond character.

#### ACKNOWLEDGMENTS

The author is grateful to Dr. Y. Inomata and Dr. Y. Sato at National Institute for Research in Inorganic Materials for stimulating discussion of the mechanical properties of materials.

<sup>1</sup>W. R. Tyson, *Philos. Mag.* **14**, 925 (1966).

<sup>2</sup>N. H. Macmillan, *J. Mater. Sci.* **7**, 239 (1972).

<sup>3</sup>A. Kelly, W. R. Tyson, and A. H. Cottrell, *Philos. Mag.* **15**, 567 (1967).

<sup>4</sup>J. R. Rice and R. Thomson, *Philos. Mag.* **29**, 73 (1974).

<sup>5</sup>W. A. Harrison, *Phys. Rev. B* **8**, 4487 (1973).

<sup>6</sup>M. Lannoo, *J. Phys. (Paris)* **40**, 461 (1979).

<sup>7</sup>M. I. Baskes, *Phys. Rev. Lett.* **59**, 2666 (1987).

<sup>8</sup>J. Tersoff, *Phys. Rev. B* **37**, 6991 (1988).

<sup>9</sup>F. H. Stillinger and T. Weber, *Phys. Rev. B* **31**, 5262 (1985).

<sup>10</sup>J. E. Sinclair, *Proc. R. Soc. London. Ser. A* **329**, 83 (1972).

<sup>11</sup>J. E. Sinclair, *Philos. Mag.* **31**, 647 (1975).

<sup>12</sup>Y. Uemura, *Phys. Status Solidi B* **167**, 51 (1991).

<sup>13</sup>M. Kohyama, R. Yamamoto, and M. Doyama, *Phys. Status*

*Solidi B* **136**, 31 (1986).

<sup>14</sup>J. C. Slater and G. F. Koster, *Phys. Rev.* **94**, 1498 (1954).

<sup>15</sup>A. A. Griffith, *Philos. Trans. R. Soc. London. Ser. A* **221**, 163 (1920).

<sup>16</sup>M. H. Grimsditch and A. K. Ramdas, *Phys. Rev. B* **11**, 3139 (1975).

<sup>17</sup>M. Mullins and M. A. Dokainish, *Philos. Mag. A* **46**, 771 (1982).

<sup>18</sup>S. Kohlhoff, P. Gumbsh, and H. F. Fischmeister, *Philos. Mag. A* **64**, 851 (1991).

<sup>19</sup>J. E. Field, in *The Properties of Natural and Synthetic Diamond*, edited by J. E. Field (Academic, New York, 1992), pp. 478-484.

<sup>20</sup>J. E. Field and C. J. Freeman, *Philos. Mag. A* **43**, 593 (1981).